What Causes Ubiquitous Earthquake Dynamic Triggering in Southern California?

Nicolas D. DeSalvio[1*], Wenyuan Fan[1], Andrew J. Barbour[2]

[1]Scripps Institution of Oceanography, UC San Diego | [2]United States Geological Survey

Poster 053 *ndesalvio@ucsd.edu NSF-EAR 2022441 and NSF GRFP DGE-2038238

1. Using Statistic Distributions to Identify Dynamic Triggering Cases

Earthquake dynamic triggering has been identified at many faults, and understanding its physical mechanisms can provide insight into earthquake nucleation and aid hazard mitigation. In this study, we systematically identify cases of dynamic triggering in Southern California from 2008-2017 and investigate possible mechanisms with a suite of geophysical observations (see DeSalvio and Fan, 2023).

We use the β-statistic to characterize seismicity-rate changes. We sample the QTM catalog to construct β-statistic distributions at the site of interest for the candidate trigger earthquakes to identify dynamic triggering cases. In addition to β, we also use the Z-statistic to identify dynamic triggering (see DeSalvio and Fan (2023) for details).

We examine every M≥6 global earthquake during the QTM catalog period at 185 grids spaced throughout southern California. Figure 1 shows an example.

$$\beta = \frac{N_a - E[N_a]}{SD[N_a]}$$

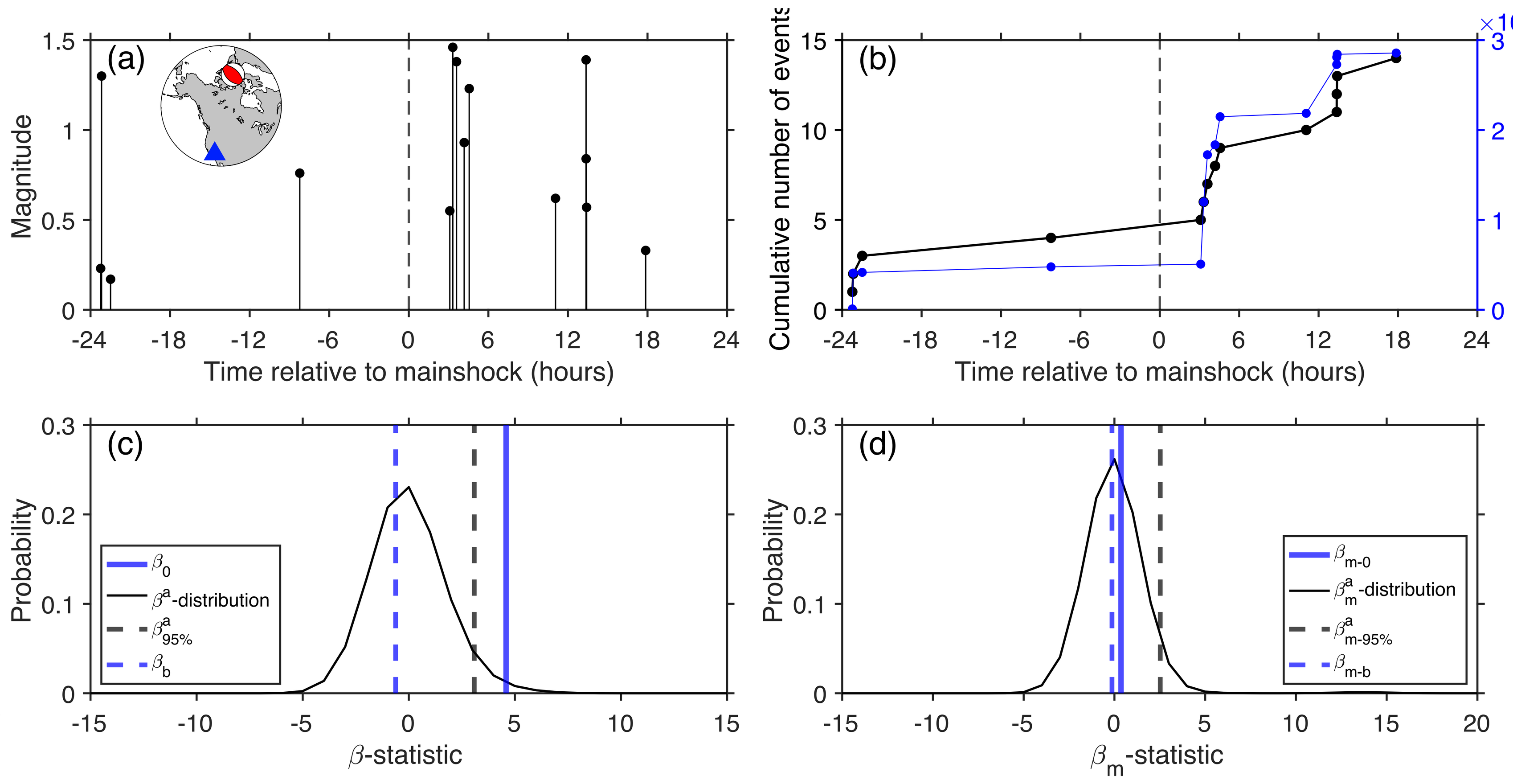

Figure 1: Seismicity and example statistic distributions at a grid near the Coso Geothermal Field after the 2017 M6 Queen Charlotte earthquake.

2. Ubiquitous Earthquake Dynamic Triggering

Triggering is Frequent. We found that 70% of remote earthquakes triggered seismicity somewhere in southern California. Triggered seismicity occurs about every 30 days to years at individual grids.

Triggering is Widespread. Figure 2 shows widespread triggering throughout southern California. The Coso Geothermal Field (CGF), Salton Sea Geothermal Field (SSGF), and San Jacinto Fault (SJF) are the most prone to triggering. About 64% of the grids considered experienced triggered seismicity.

Triggering is Delayed. Most cases of dynamic triggering occur several hours after the seismic waves from the distant earthquake pass through California. **This indicates that the underlying processes are time-dependent.**

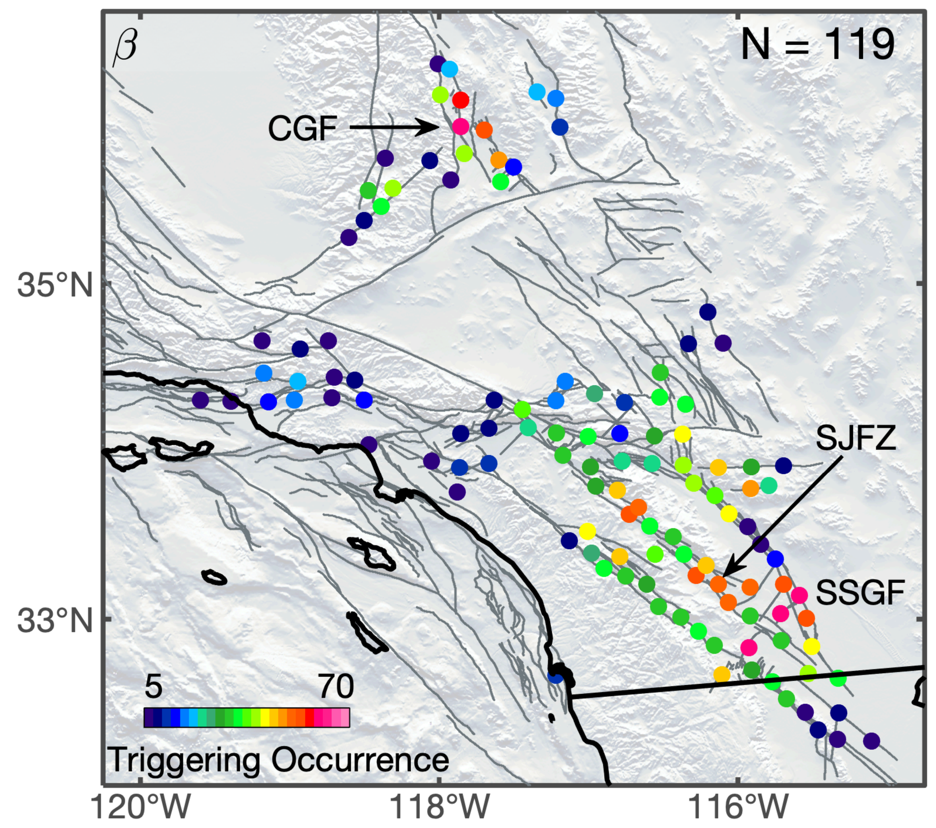

Figure 2: Spatial triggering patterns in southern California. Triggering occurrence is the number of candidate trigger earthquakes that caused seismicity in any of the tested time windows. N denotes the number of triggered grids.

3. Significant Triggered Moment Release

Here we also develop a new statistic, β_m, to identify moment release anomalies, revealing when and where larger-than-expected earthquakes were triggered. As small earthquakes have negligible moment-release, β_m is less dependent on the magnitude of completeness than β.

Anomalous seismic moment-release is less commonly observed than seismicity rate changes. However, it is still widespread and frequent. We observe moment-release anomalies at over 50% of the grids and after about 52% of the remote earthquakes.

$$\beta_m = \frac{M_a - E[M_a]}{SD[M_a]} \quad M_a = \sum_{i=1}^{N_a} 10^{1.5m_i + 9.1}$$

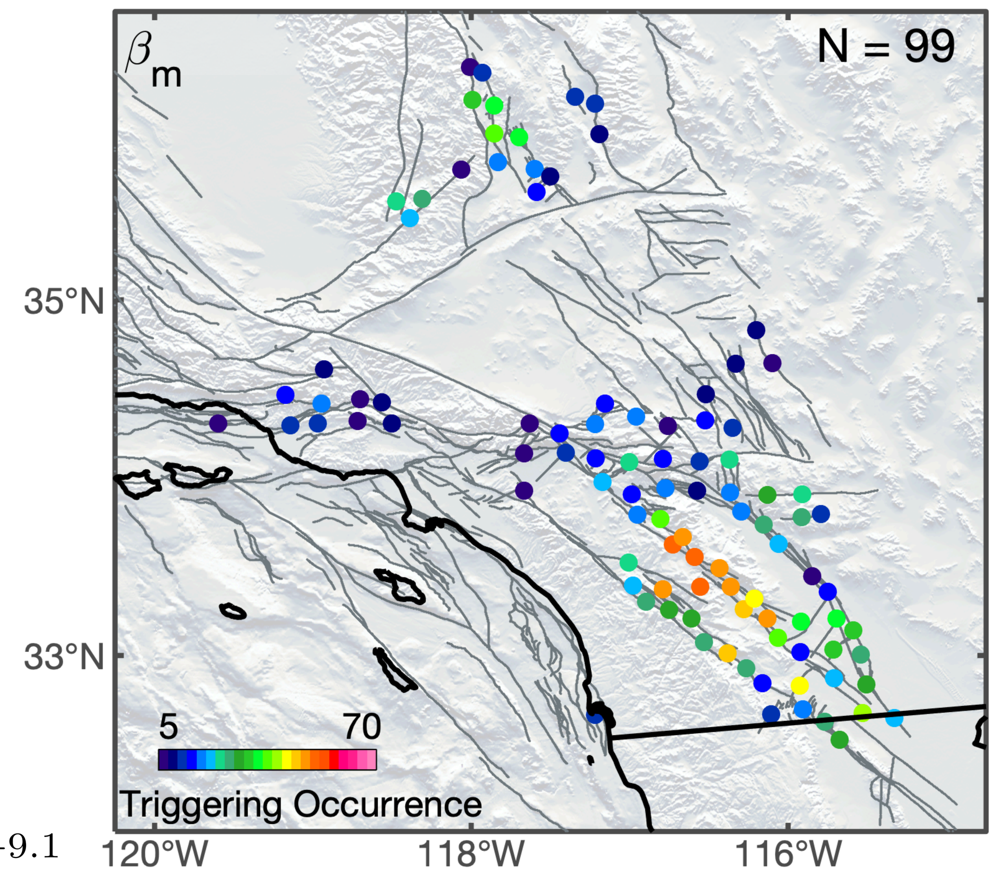

Figure 3: Moment release anomaly occurrence in southern California.

4. Is Anything Unique About the Passing Waves?

We analyze velocity waveforms of candidate trigger earthquakes in southern California and measure four instantaneous waveform metrics. The metrics are peak ground velocity in two frequency bands, peak frequency, kinetic energy, and relative frequency content (FCR, see below).

The metrics are computed for each seismic station in the study area independently, and the measurements for each candidate trigger earthquake at a given grid are interpolated from nearby stations. The resulting values are shown in Figure 4, colored by the triggering result at that grid and time for comparison.

The waveform characteristics do not appear to deterministically differentiate the triggering incidences from non-triggering cases or separate instantaneous and delayed cases. This confirms that there is no simple triggering threshold and suggests that the relevant processes are nonlinear.

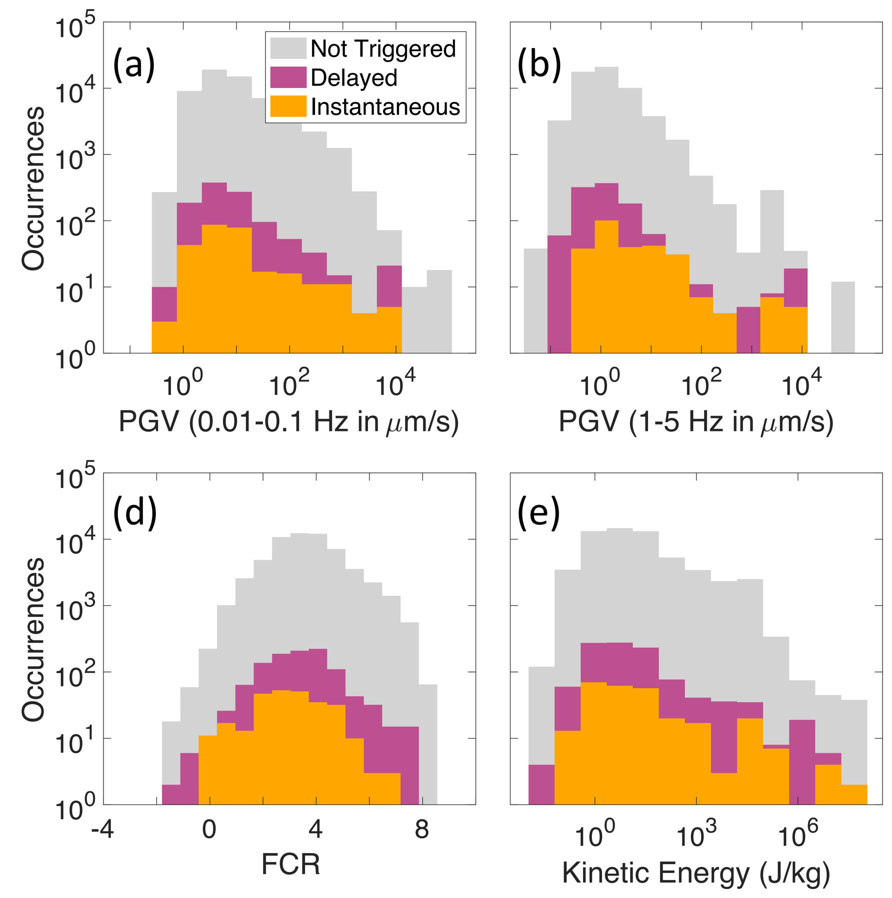

Figure 4: Distributions of peak ground velocity (a-b), peak frequency (c), relative frequency content (d), and kinetic energy (e)

$$\mathrm{FCR} = \log_{10}\left(\frac{\int_{f_{0.1}}^{f_1} S(f)\,df}{\int_{f_1}^{f_5} S(f)\,df}\right)$$

where $S(f)$ is the power spectrum

5. Triggering is Local

We estimate the relevant length scale of the triggering processes by examining concurrent triggering at nearby locations after the same earthquake. We have developed a metric termed the synchronization coefficient:

$$S_{ij} = \frac{N_{shared}}{N_{total}}$$

Where N_{shared} is the number of remote earthquakes that triggered *both* grids and N_{total} is the number of remote earthquakes that triggered *one or both* grids.

We hypothesize that high S values reflect similar triggering processes at the grids, and the pairwise distance is a proxy for the spatial extent of the process. Figure 5 shows that high values of S drop off after a pairwise distance of 40 km. Given our gridding scheme, all grids that are less than 40km apart overlap. **We infer that the triggering processes are local, acting on length scales less than 40km.**

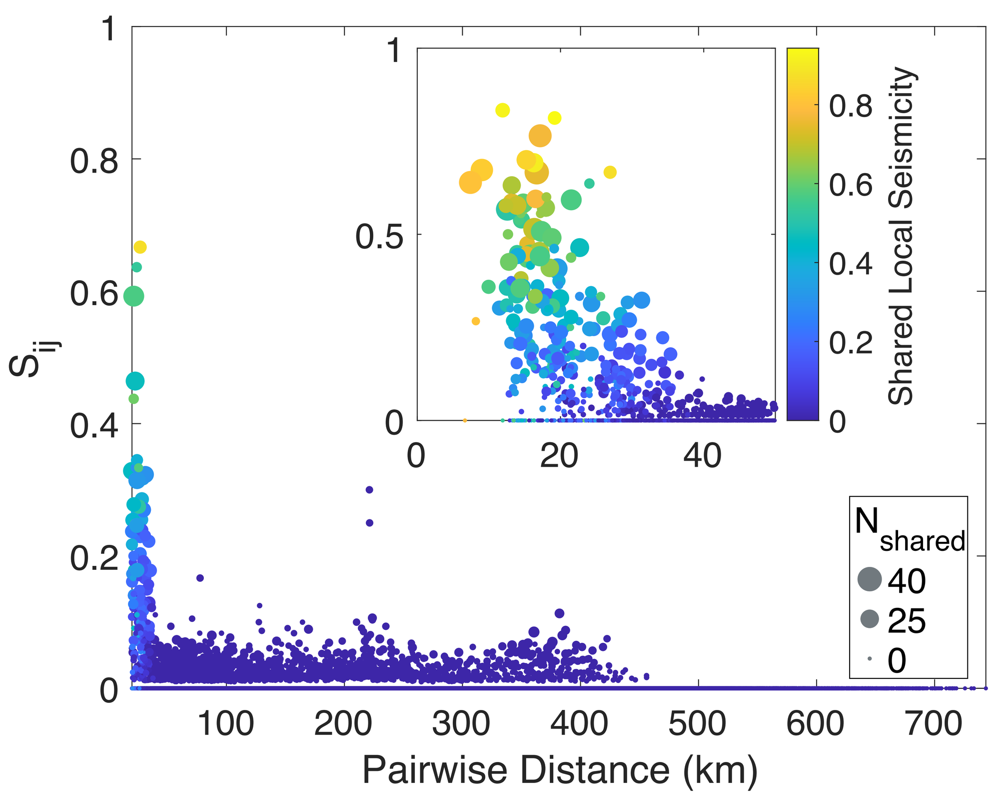

Figure 5: Synchronization coefficient versus pairwise grid node distance.

6. Duration of Dynamic Strain: A New Metric?

Time-dependent, nonlinear, local processes seem to have a primary role in regulating dynamic triggering. To explore one such process, we use Network of the Americas strain data in Anza to estimate strain duration at various critical strain values. The strain duration relates to cyclic loading from the seismic waves and energy dissipation: elevated and sustained levels of strain duration may facilitate crack development and growth, eventually triggering earthquakes. Using synthetic seismograms, Pollitz et al. 2012 found that the 2012 Indian Ocean Earthquake triggered seismicity at sites with strain above 100ns for 100 seconds. To test this hypothesis, we use strainmeter data to calculate the duration of the RMS strain curve above several thresholds and will compare the results with the triggering identifications. Figures 6 and 7 demonstrate an example of this calculation.

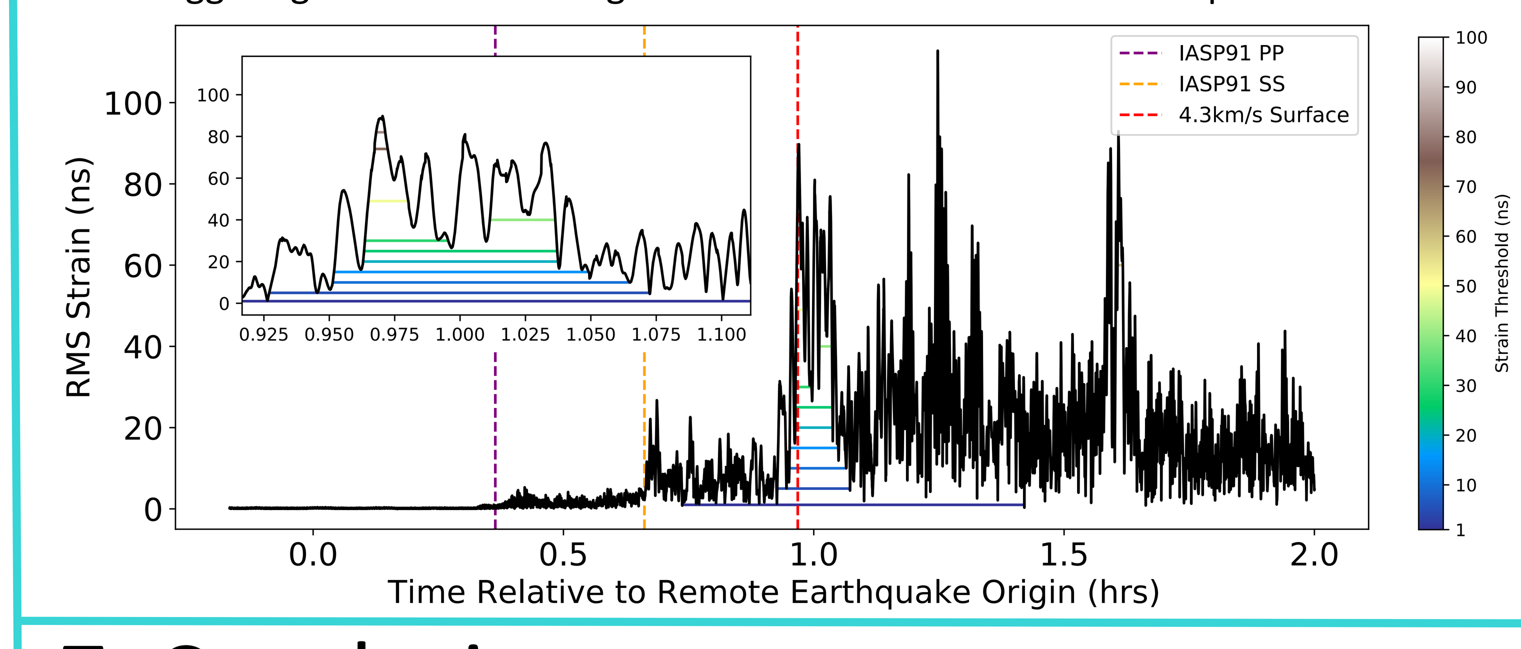

Figure 6 (left): RMS strain curve at Anza station B084 following the 2012 Indian Ocean earthquake. Colored horizontal lines indicate the duration values at various strain thresholds.

Figure 7 (right): The resulting strain threshold vs duration curve corresponding to Figure 6.

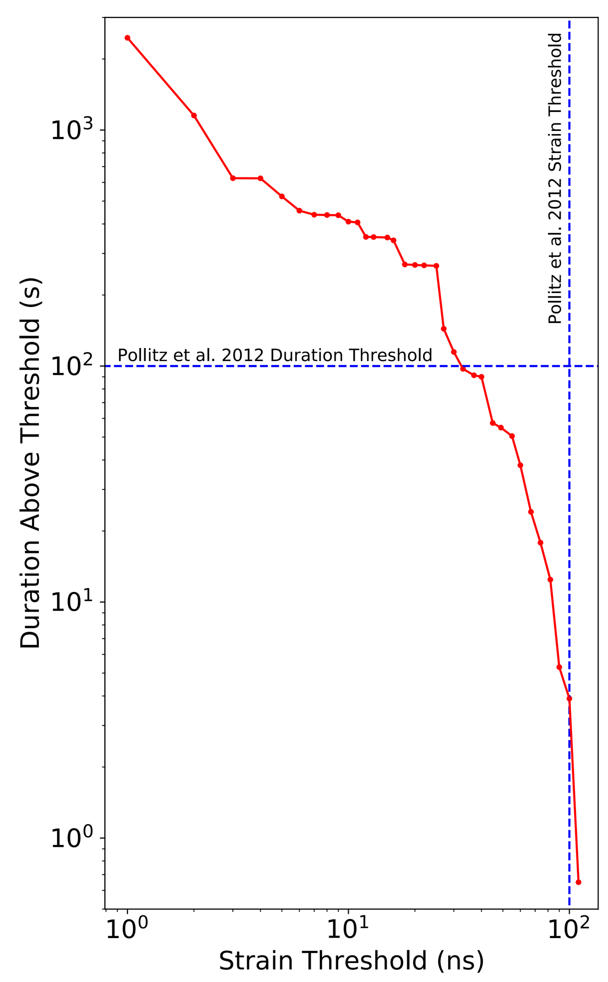

7. Conclusions

- Earthquake dynamic triggering is frequent and widespread in southern California.
- Significant moment-release anomalies occur less often than significant seismicity-rate increases but are still frequent and widespread.
- Analyses of triggering patterns and waveform data suggest that the triggering processes are time-dependent, nonlinear, and at local scales.

What's Next?

- Systematically evaluate the strain duration hypothesis.
- Apply the methodology in different tectonic regions to comparatively investigate the local-scale results.

DeSalvio, N. D., & Fan, W. (2023). Ubiquitous Earthquake dynamic triggering in southern California. *Journal of Geophysical Research: Solid Earth*, 128, e2023JB026487.

Pollitz, F. F., Stein, R. S., Sevilgen, V., & Bürgmann, R. (2012). The 11 April 2012 east Indian Ocean earthquake triggered large aftershocks worldwide. *Nature, 490*(7419), 250–253.